

## Nonlinear Micromechanical Casimir Oscillator

H. B. Chan,\* V. A. Aksyuk, R. N. Kleiman, D. J. Bishop, and Federico Capasso†

*Bell Laboratories, Lucent Technologies, Murray Hill, New Jersey 07974*

(Received 25 June 2001; published 31 October 2001)

The Casimir force between uncharged metallic surfaces originates from quantum-mechanical zero-point fluctuations of the electromagnetic field. We demonstrate that this quantum electrodynamical effect has a profound influence on the oscillatory behavior of microstructures when surfaces are in close proximity ( $\leq 100$  nm). Frequency shifts, hysteretic behavior, and bistability caused by the Casimir force are observed in the frequency response of a periodically driven micromachined torsional oscillator.

DOI: 10.1103/PhysRevLett.87.211801

PACS numbers: 12.20.Fv, 05.45.-a, 07.10.Cm

Casimir forces are interactions between electrically neutral and highly conductive metals [1,2]. They are regarded as one of the most striking manifestations of quantum fluctuations. The boundary conditions imposed on the electromagnetic fields lead to a spatial redistribution of the mode density with respect to free space, creating a spatial gradient of the zero-point energy density and hence a net force between the metals.

The last few years have witnessed a resurgence of experiments [3–5] on these forces following the high precision measurements by Lamoreaux [6] using a torsional pendulum. Pioneering measurements were performed by Sparnaay [7] followed later by the work of Van Blokland and Overbeek [8] who accurately verified the existence of the Casimir effect. Between two parallel plates, the Casimir force is attractive and assumes the form  $F_c = -\pi^2 \hbar c S / 240 z^4$ , where  $c$  is the speed of light,  $\hbar$  is Planck constant/ $2\pi$ ,  $S$  is the area of the plates, and  $z$  is their separation. In practice, one of the interacting surfaces is usually chosen to be spherical to avoid alignment problems, modifying the force to  $F_{cs} = -\pi^3 \hbar c R / 360 z^3$ , where  $R$  is the radius of the sphere [9].

Casimir forces are inherently mesoscopic in nature since they can acquire substantial values when the separation between the metallic surfaces is reduced to  $\leq 100$  nm. In addition, because of their topological nature associated with the dependence on the boundary conditions of the electromagnetic fields, their spatial dependence and sign can be controlled by tailoring the shapes of the interacting surfaces [10]. The above considerations have motivated us to investigate the effect of these quantum electrodynamical forces on the mechanical properties of artificial microstructures. Microelectromechanical systems (MEMS) [11] are ideally suited for these studies because their moving parts can be engineered with high precision using state-of-the-art silicon integrated circuits technology and their separation can be controlled with high accuracy down to submicron distances [12].

In a previous paper we demonstrated the effect of the Casimir force on the *static* properties of micromechanical systems [5]. We used the deflection of a micromachined plate by a microsphere for a high precision measurement of

the Casimir force. Other studies have focused on adhesion and sticking of mobile parts in MEMS due to the Casimir effect [13]. In this Letter we show that Casimir interactions have a profound effect on the *dynamic* properties of microstructures. In particular, we report on the experimental realization of a forced micromechanical nonlinear oscillator in which the anharmonic behavior arises solely from the Casimir effect. A similar oscillator had been proposed and theoretically analyzed by Serry, Walliser, and Maclay [12]. While there is vast experimental literature on the hysteretic response and bistability of nonlinear oscillators in the context of quantum optics, solid-state physics, mechanics, and electronics, the experiment described in this Letter represents, to our knowledge, the first observation of bistability and hysteresis caused by a quantum electrodynamical effect.

A simple model of the Casimir oscillator consists of a movable metallic plate subjected to the restoring force of a spring obeying Hooke's law and the nonlinear Casimir force arising from the interaction with a fixed metallic sphere (Fig. 1 inset). For separations  $d$  larger than a critical value [12], the system is bistable: the potential energy consists of a local minimum and a global minimum separated by a potential barrier (Fig. 1). The local minimum is a stable equilibrium position, about which the plate undergoes small oscillations. The Casimir force modifies the curvature of the confining potential around the minimum, thus changing the natural frequency of oscillation and also introduces high order terms in the potential, making the oscillations anharmonic.

We realize such an oscillator making use of MEMS technology. The micromachined oscillator consists of a  $3.5\text{-}\mu\text{m}$ -thick,  $500\text{-}\mu\text{m}^2$  polysilicon plate (metallized on the top with gold) free to rotate about two torsional rods on opposite edges (right inset in Fig. 2). The fabrication steps of a similar device used to study static effects of Casimir forces are described in Ref. [5]. We excite the torsional mode of oscillation by applying a driving voltage to one of the two electrodes that is fixed in position under the plate (left inset in Fig. 2). The driving voltage is a small ac excitation  $V_{ac}$  with a dc bias  $V_{dc1}$  to linearize the voltage dependence of the driving torque. The top plate is

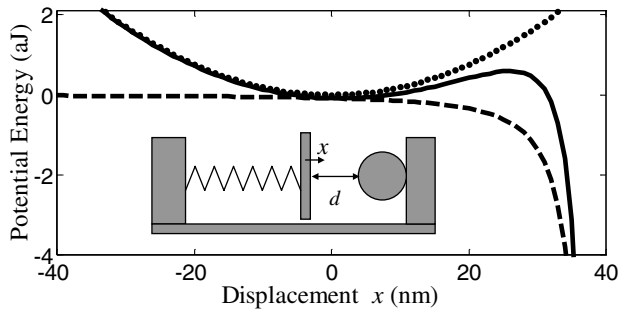


FIG. 1. Inset: a simple model of the nonlinear Casimir oscillator (not to scale). Main figure: elastic potential energy of the spring (dotted line, spring constant =  $0.019 \text{ N m}^{-1}$ ), energy associated with the Casimir attraction (dashed line) and total potential energy (solid line) as a function of plate displacement. The distance  $d$ , measured between the sphere ( $100 \mu\text{m}$  radius) and the equilibrium position of the plate in the absence of the Casimir force, is chosen to be  $40 \text{ nm}$ .

grounded while the detection electrode is connected to a dc voltage  $V_{dc2}$  through a resistor. Oscillatory motion of the top plate leads to a time varying capacitance between the top plate and the detection electrode. For small oscillations, the change in capacitance is proportional to the rotation of the plate. The detection electrode is connected to an amplifier and a lock-in amplifier measures the output signal at the excitation frequency.

The measurement is performed at room temperature and at a pressure of less than  $1 \text{ mtorr}$ . Despite the soft torsional spring constant ( $k = 2.1 \times 10^{-8} \text{ N m rad}^{-1}$ ), the resonance frequency of the torsional mode is maintained reasonably high due to the small moment of inertia ( $I = 7.1 \times 10^{-17} \text{ kg m}^2$ ) of the top plate. The resonance peaks of the oscillator for different excitation voltages (Fig. 2) are fitted very well by the black curves representing driven motions of a damped harmonic oscillator. As expected, the resonance frequency remains constant at  $2753.47 \text{ Hz}$ , while the peak oscillation amplitude increases linearly with excitation. This clearly demonstrates that the

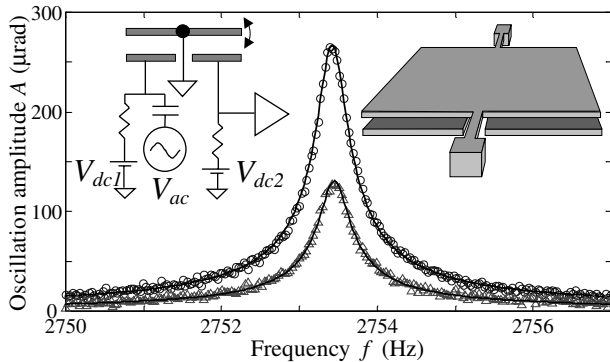


FIG. 2. Resonance peaks of the torsional oscillator at excitation voltage amplitudes of  $35.4 \mu\text{V}$  (triangles) and  $72.5 \mu\text{V}$  (circles). The solid lines are fits to the data based on a driven harmonic oscillator. Inset (right): schematic of the torsional oscillator (not to scale). Inset (left): cross section of the device with the electrical connections and measurement circuit.

oscillator behaves linearly in the absence of forces from external objects.

To investigate the effect of the Casimir force on the oscillator, we placed a  $200\text{-}\mu\text{m}$ -diameter polystyrene sphere (metallized with gold) close to one side of the oscillator (Fig. 3 inset). The distance  $z$  between the sphere and the equilibrium position of the top plate (i.e., without the periodic driving torque) is varied by a closed-loop piezoelectric stage. In the presence of the sphere, the equation of motion for the oscillator is given by

$$\ddot{\theta} + 2\gamma\dot{\theta} + [\omega_0^2 - (b^2/I)F'(z)]\theta = (\tau/I)\cos\omega t - \alpha\theta^2 - \beta\theta^3, \quad (1)$$

where  $\tau$  is the amplitude of the driving torque,  $b$  is the lateral distance of the sphere from the center of the top plate,  $\omega_0 = \sqrt{k/I}$  is the fundamental frequency of the oscillator,  $\gamma$  is the damping coefficient,  $\alpha = b^3 F''(z)/2I$  and  $\beta = -b^4 F'''(z)/6I$ .  $F'(z)$ ,  $F''(z)$ , and  $F'''(z)$  denote the first, second, and third spatial derivatives of the external force  $F$ , respectively, evaluated at distance  $z$ . In our experiment,  $F$  is either the Casimir force or an applied electrostatic force between the sphere and the top plate. To obtain Eq. (1),  $F(z - b\theta)$  has been Taylor expanded about  $z$  up to  $\theta^3$ . For small oscillations where the nonlinear terms  $\theta^2$  and  $\theta^3$  can be neglected, the external force modifies the mechanical resonance frequency of the oscillator by an amount that is proportional to the force gradient:

$$\omega_1 = \omega_0[1 - b^2 F'(z)/2I\omega_0^2]. \quad (2)$$

To calculate  $b$ , we deliberately apply a voltage to the sphere to set up an electrostatic force gradient. Then we record the change in resonance frequency of the oscillator as we vary the distance  $z$  by changing the piezoextension. The gradient of the electrostatic force  $F_e$  between the sphere and the top plate is given by

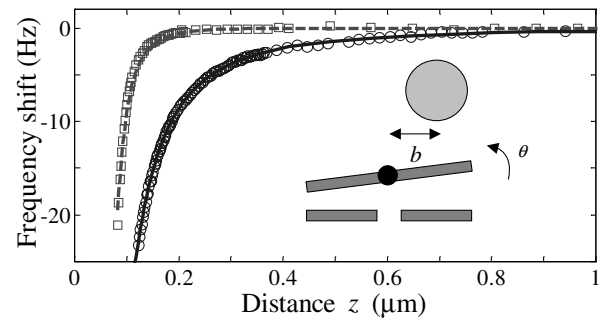


FIG. 3. Change in resonance frequency of the oscillator in response to the electrostatic force (circles,  $V = 408.5 \text{ mV}$ ) and Casimir force (squares) as a function of distance. The amplitude of the excitation is  $8.2 \mu\text{V}$ , producing oscillations of the plate with an amplitude of  $5.8 \text{ nm}$  at its closest point to the sphere. The solid and dashed lines are fits obtained with Eqs. (3) and (4), respectively. Inset: schematic of the experiment (not to scale). The oscillation angle  $\theta$  indicated by the curved arrow is measured from the equilibrium position of the plate in the absence of driving torque.

$$F'_c(z) = \epsilon_0 \pi R (V - V_0)^2 / (\Delta z + z_0)^2 \quad \text{for } \Delta z + z_0 \ll R, \quad (3)$$

where  $\epsilon_0$  is the permittivity of vacuum,  $R$  is the radius of the sphere,  $V$  is the voltage applied to the sphere,  $V_0$  is the residual voltage on the sphere,  $z_0$  is the distance of closest approach of the sphere from the plate, and  $\Delta z$  is the separation between the sphere and plate measured from  $z_0$ , so that  $z = \Delta z + z_0$ . Here  $z_0$  is not the minimum achievable separation. While it is possible to extend the piezo further to decrease the value of  $z_0$ , we did not attempt to do so in order to prevent the top plate of the oscillator from jumping into contact with the sphere. The residual voltage  $V_0$  arises from the work function difference of the two gold surfaces (on the sphere and on the top plate) as a result of slight variations in the preparation of the films [5,8].  $V_0$  is found to be 75 mV by fixing the distance  $z$  and identifying the voltage  $V$  at which the maximum of the quadratic voltage dependence of the resonance frequency occurs.

We perform a fit of the resonance frequency shift of the oscillator (solid line in Fig. 3) in response to the electrostatic force gradient using Eqs. (2) and (3) with  $z_0$  and  $b$  as fitting parameters (determined to be 122.4 nm and 131.0  $\mu\text{m}$ , respectively). We then set the voltage  $V$  on the sphere equal to the residual voltage  $V_0$  to eliminate the electrostatic contributions to the force gradient. In Fig. 3, the squares are the shifts in resonance frequency obtained when we repeat the measurement with  $V = V_0$ . The dashed line is a fit to the predicted frequency shift [Eq. (2)] due to the Casimir force gradient assuming perfectly conducting surfaces:

$$F'_{cs}(z) = \pi^3 \hbar c R / 120 (\Delta z + z_1)^4, \quad (4)$$

where  $z_1$  is the distance of the sphere from the plate at the distance of closest approach (determined to be 85.9 nm from the fit). As we discussed in an earlier experiment [5], for an exact comparison of data with theory the finite conductivity and surface roughness of the metal films must be taken into account [14]. However, we do not attempt such a precise comparison here because contributions from the higher order derivatives of the Casimir force modify the shift calculated from Eq. (2) by more than 5% at the smallest separations, as we discuss later. As a result the uncertainty in deducing the Casimir force from the measured frequency shift [using Eq. (2)] is in excess of 5% at the closest separation. This value is significantly larger than the experimental error in our earlier static measurement ( $\leq 1\%$ ). However, in the linear regime dynamic techniques are expected to ultimately yield a higher sensitivity than static measurements [15].

To demonstrate the nonlinear effects introduced by the Casimir force, we first retract the piezo until the sphere is more than 3.3  $\mu\text{m}$  away from the oscillating plate so that the Casimir force has a negligible effect on the oscillations. The measured frequency response shows a resonance peak

that is characteristic of a driven harmonic oscillator (peak I in Fig 4a), regardless of whether the frequency is swept up (hollow squares) or down (solid circles). This ensures the excitation voltage is small enough so that intrinsic nonlinear effects in the oscillator are negligible in the absence of the Casimir force. We then extend the piezo to bring the sphere close to the top plate while maintaining the excitation voltage at fixed amplitude. The resonance peak shifts to lower frequencies (peaks II, III, and IV), by an amount that is consistent with the distance dependence in Fig. 3. Moreover, the shape of the resonance peak deviates from that of a driven harmonic oscillator and becomes asymmetric. As the distance decreases, the asymmetry becomes stronger and hysteresis occurs. This reproducible hysteretic behavior is characteristic of strongly nonlinear oscillations [16]. For a given excitation  $\tau$  and frequency  $\omega$ , the amplitude of oscillation  $A$  is given by the roots of the following equation:

$$A^2[(\omega - \omega_1 - \kappa A^2)^2 + \lambda^2] = \tau^2 / 4I^2 \omega_1^2, \quad (5)$$

where  $\kappa = 3\beta/8\omega_1 - 5\alpha^2/12\omega_1^3$  characterizes the nonlinear effects. When the nonlinearity is weak, Eq. (5) has only a single positive solution for  $A^2$ . In the presence of strong nonlinearity, such as those introduced by the Casimir force in our experiment, the oscillation amplitude  $A$  becomes triple valued for a range of frequency, corresponding to the three positive roots of  $A^2$  in Eq. (5). The solid lines in Fig. 4a show the predicted frequency response of the oscillator with  $\omega_1$  and  $\kappa$  determined by the first, second, and third spatial derivatives of the Casimir

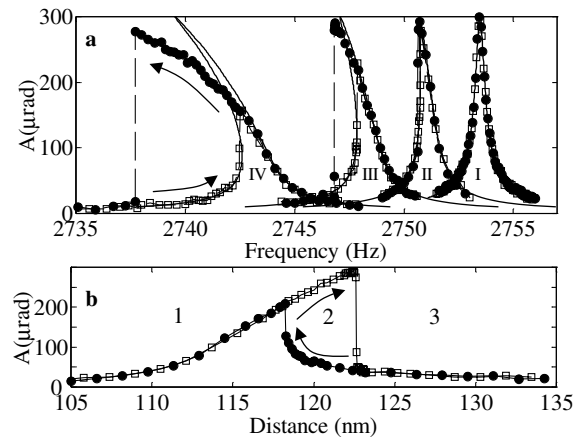


FIG. 4. (a) Hysteresis in the frequency response induced by the Casimir force on an otherwise linear oscillator. Hollow squares (solid circles) are recorded with increasing (decreasing) frequency. The distance  $z$  between the oscillator and the sphere is 3.3  $\mu\text{m}$ , 141 nm, 116.5 nm, and 98 nm for peaks I, II, III, and IV, respectively. The excitation amplitude is maintained constant at 55.5  $\mu\text{V}$  for all four separations. The solid lines are the calculated response using Eq. (5), with  $\kappa = 0$ ,  $-3.1 \times 10^7$ ,  $-1.0 \times 10^8$ , and  $-2.8 \times 10^8 \text{ rad}^{-2} \text{ s}^{-1}$  for peaks I, II, III, and IV, respectively. The peak oscillation amplitude for the plate is 39 nm at its closest point to the sphere. (b) Oscillation amplitude as a function of distance with excitation frequency fixed at 2748 Hz.

force at  $z = 98$  nm, 116.5 nm, 141 nm, and  $3.3 \mu\text{m}$ , respectively. The values of other parameters ( $\gamma, b, I, \tau$ ) are identical for all four resonance peaks. At a particular distance, the spatial derivatives of the Casimir force determine both the frequency and the shape of the resonance peaks without any other adjustable parameters. Indeed, the shape and the frequency of peaks II and III agree well with Eq. (5). For peak IV, the hysteretic effects are very strong and deviations from Eq. (5) become apparent. This discrepancy arises from contributions of higher order spatial derivatives that we neglected in the series expansion of the Casimir force [Eq. (1)], as well as corrections to the Casimir force as a result of finite conductivity and roughness of the surfaces [14].

An alternative way to demonstrate the “memory” effect of the oscillator is to maintain the excitation at a fixed frequency and vary the distance between the sphere and the plate (Fig. 4b). As the distance changes, the resonance frequency  $\omega_1$  of the oscillator shifts, to first order because of the changing force gradient [Eq. (2)]. In region 1, the fixed excitation frequency is higher than the resonance frequency and vice versa for region 3. In region 2, the amplitude of oscillation depends on the history of the plate position. Depending on whether the plate was in region 1 or region 3 before it enters region 2, the amplitude of oscillation differs by up to a factor of 6. This oscillator therefore acts as a sensor for the separation between the two surfaces.

In Fig. 4a, we used a constant quality factor  $Q = 7150$  to fit all four resonance peaks at different distances. Further improvements in sensitivity could enable us to explore possible changes in  $Q$  with distance. There has been an interesting prediction [17] that dissipative retarded van der Waals forces can arise between surfaces in relative motion due to the exchange of virtual photons which couple to acoustic phonons in the material. Similar dissipative Casimir forces can arise between metals; here virtual photons would couple to particle-hole excitations in the metal [18]. This would lead to changes in the  $Q$  of our oscillator with position. It is also interesting to point out that the nonuniform relative acceleration of the metal and the sphere will lead, at least in principle, to an additional damping mechanism associated with the parametric down-conversion of vibrational quanta into pairs of photons, a quantum electrodynamical effect associated with the nonlinear properties of vacuum. This phenomenon, which was investigated theoretically by Lambrecht, Jackel, and Reynaud in the context of a vibrating parallel plate capacitor [19], is an example of the so called dynamical Casimir effect, i.e., the nonthermal radiation emitted by uncharged dielectric bodies in a state of nonuniform acceleration [20]. Although this effect is completely negligible in our system, it does represent a fundamental lower limit to the damping of the Casimir oscillator.

Finally, we remark that nonlinear effects in a mechanical oscillator arising from ordinary electrostatic forces were studied by several groups [21,22]. In particular, Buks and

Roukes [22] considered the role of the Casimir force in such nonlinear oscillators. While the relative strength of the electrostatic force to the Casimir force was not given, using their smallest separation of  $0.77 \mu\text{m}$  and 30 V between the surfaces we estimate that in their experiment the Casimir force is roughly  $10^6$  times smaller than the electrostatic force before pull-in assuming a simple parallel plate model. Therefore, quantum effects such as the Casimir force have a negligible effect on the nonlinearity observed in their oscillator, though the pull-in and sticking of their oscillator might in part be due to the Casimir force.

We thank L. S. Levitov, M. Schaden, L. Spruch, R. Onofrio, M. R. Andrews, D. Abusch-Magder, R. de Picciotto, M. I. Dykman, C. F. Gmachl, A. Moustakas, L. N. Pfeiffer, P. M. Platzman, and N. Zhitenev for assistance and useful discussions.

---

\*Electronic address: hochan@lucent.com

†Electronic address: fc@lucent.com

- [1] H. B. G. Casimir, Proc. K. Ned. Akad. Wet. **51**, 793 (1948).
- [2] For comprehensive reviews, see P. W. Milonni and M. L. Shih, Contemp. Phys. **33**, 313 (1992); L. Spruch, Science **272**, 1452 (1996); V. M. Mostepanenko and N. N. Trunov, *The Casimir Effect and Its Applications* (Oxford, New York, 1997).
- [3] U. Mohideen and A. Roy, Phys. Rev. Lett. **81**, 4549 (1998); A. Roy and U. Mohideen, Phys. Rev. Lett. **82**, 4380 (1999).
- [4] T. Ederth, Phys. Rev. A **62**, 062104 (2000).
- [5] H. B. Chan *et al.*, Science **291**, 1941 (2001).
- [6] S. K. Lamoreaux, Phys. Rev. Lett. **78**, 5 (1997); Am. J. Phys. **67**, 850 (1999).
- [7] M. J. Sparnaay, Physica (Utrecht) **24**, 751 (1958).
- [8] P. H. G. M. Van Blokland and J. T. G. Overbeek, J. Chem. Soc. Faraday Trans. I **74**, 2637 (1978).
- [9] B. V. Derjaguin and I. I. Abrikosova, Sov. Phys. JETP **3**, 819 (1957).
- [10] T. H. Boyer, Phys. Rev. **174**, 1764 (1968); P. W. Milonni and P. B. Lerner, Phys. Rev. A **46**, 1185 (1992).
- [11] W. S. Trimmer, *Micromechanics and MEMS: Classic and Seminal Papers to 1990* (IEEE Press, New York, 1997).
- [12] F. M. Serry, D. Walliser, and G. J. Maclay, J. Microelectromech. Syst. **4**, 193 (1995).
- [13] E. Buks and M. L. Roukes, Phys. Rev. B **63**, 033402 (2001).
- [14] G. L. Klimchitskaya *et al.*, Phys. Rev. A **60**, 3487 (1999).
- [15] G. Bressi *et al.*, Classical Quantum Gravity **18**, 3943 (2001).
- [16] L. D. Landau and E. M. Lifshitz, *Mechanics* (Pergamon, New York, 1976).
- [17] L. S. Levitov, Europhys. Lett. **8**, 499 (1989).
- [18] L. S. Levitov (private communication).
- [19] A. Lambrecht, M. Jackel, and S. Reynaud, Phys. Rev. Lett. **77**, 615 (1996).
- [20] S. A. Fulling and P. C. W. Davies, Proc. R. Soc. London A **348**, 393 (1976); J. Schwinger, Proc. Natl. Acad. Sci. U.S.A. **90**, 958 (1993).
- [21] H. Krömmmer *et al.*, Europhys. Lett. **50**, 101 (2000).
- [22] E. Buks and M. L. Roukes, Europhys. Lett. **54**, 220 (2001).